Journal of Thermal Analysis and Calorimetry, Vol. 66 (2001) 47–57

Mg–Ce ALLOYS
Experimental investigation by Smith thermal analysis

A. Saccone[1], *D. Macciò*[1], *S. Delfino*[1], *F. H. Hayes*[2] *and R. Ferro*[1]

[1]Dipartimento di Chimica e Chimica Industriale, Sezione di Chimica Inorganica e Metallurgia, Università di Genova, Genova, Italy
[2]Materials Science Centre, University of Manchester and UMIST, Manchester, United Kingdom

Abstract

The magnesium-cerium system has been partially revised in the Ce-rich and Mg-rich regions by using results obtained with the Smith thermal analysis (STA) technique. Nine alloys were examined and, after the thermal measurements, were subjected to phase analysis by means of X-ray powder diffraction (XRD), optical (LOM) and scanning electron microscopy (SEM), and electron probe microanalysis (EPMA). The coordinates of the invariant reactions, many of them very close to each other, were established and compared with literature data where a call for a deeper investigation was proposed as the thermal values were open to different interpretations.

Keywords: magnesium alloys, rare earth alloys, Smith thermal analysis

Introduction

For the experimental determination of phase diagrams the use of different techniques can be beneficial. The role of thermal analysis has been of primary importance since the beginning of this research field, as has been pointed out by different authors (see on this topic, for instance, [1–3] and the recent review by Ferro *et al.* [4]).

Traditional thermal analysis presents several advantages, compared to the more modern differential thermal analysis techniques, e.g. a good precision of temperature values. However, there can be a certain decreased sensitivity, leading to the lack of transitions to which small thermal effects are associated. This reason, along with the insufficient definition in some points (e.g. when a monovariant curve is crossed), led to the greater diffusion of the DTA and DSC techniques, now the standard thermal analysis methods in phase diagram investigation of metallic systems, for which small (or very small) samples may be routinely used. However, other techniques ought to be used, in particular, when a better precision in temperature data is necessary or two or more thermal effects occur over a very narrow temperature interval. In a DTA run, in fact, the onset of the peak associated with a thermal effect corresponds to an increasing difference between the sample and reference temperatures, thus accelerating the process to which the peak is associated, just when it should be slower to allow the completion of the reactions to maintain equilibrium conditions. In some of the cases

1418–2874/2001/ $ 5.00
Akadémiai Kiadó, Budapest

in which two thermal effects occur in a narrow temperature range, this does not allow the first transformation to go to completion before the onset of the subsequent one (this may be especially relevant in the case of peritectic or solid state transformations). Moreover, the 'tailing' of the corresponding peak can affect or even completely mask the peak corresponding to the second effect ('masking effect'). Some drawbacks can be overcome, by using the technique described in [5], according to which the alloy is annealed, inside the DTA apparatus, a few degrees below the expected peak, on heating (or above the peak, on cooling).

Otherwise, the technique suggested by Smith [6] and subsequently improved [7, 8] can be used, in which the temperature difference between the sample and the internal wall of the furnace, instead of the heating and cooling rate as in the DTA, is maintained constant. The measurement is performed in a furnace with low thermal mass, thereby giving the quick response demanded by the system program. The rate is governed by the value of (T_f–T_s), a constant value of which is imposed by the controller (T_f is the temperature of the internal wall of the furnace and T_s the sample temperature). On the basis of the conditions assumed, when C_p is nearly constant and no transformation takes place in the sample, a nearly constant heating rate will be obtained. On the other hand, when for instance an invariant reaction takes place and the sample temperature tends to remain constant, a decrease in the heating rate will result from the controller action in order to maintain the pre-imposed T_f–T_s value constant. An amplification of the characteristic 'temperature halt' will be obtained and the completeness of the reaction will be favoured. As the temperature remains almost constant until the process is complete, the 'envelopment' phenomena, very frequent for peritectic processes, are overcome, thus reducing spurious peaks due to 'out of equilibrium' processes. When a monovariant equilibrium line is crossed, the specific heat variation produces a more or less sharp variation of the baseline slope.

The drawbacks of this method are connected with the great slowness of the measurement and the presence of additional effects due to the high sensitivity of the apparatus, which sometimes requires a repetition of the measurements. On the other hand, the method presents the advantages of a very high sensitivity and the ability to separate peaks at very close temperatures. Moreover, it is possible to detect solid state reactions with smaller hysteresis effects (these are usually present when DTA is used), provided that ΔH of the transformation is high enough.

This technique is mainly a check and refinement tool, to be coupled with other thermal analysis techniques, e.g. DTA, and with theoretical forecast methods. The technique has been used in the Materials Science Centre at the University of Manchester and UMIST (UK) to investigate several alloy systems, for instance, Al-alloys [7, 9, 10], Au-alloys [8, 9, 11], In–Cd alloys [12] and Ag–Cd–In alloys [13, 14]. Moreover, some relevant parts of the Mg–Pr phase diagram were studied in co-operation with the University of Genova (Italy), with a partially modified instrument described in [15].

This paper concerns a re-investigation of the phase equilibria in the Mg–Ce system for which several data reported in literature, mostly temperatures of invariant reactions, are not unequivocal.

Magnesium-rare earth systems: literature data

The binary systems formed by magnesium with the rare earth metals (R) have been thoroughly studied by our research group working in Genova University using the conventional DTA method. They are: Nd–Mg [16], Pr–Mg [17], Sm–Mg [18], Tb–Mg [19], Dy–Mg [20], Ho–Mg [21], Er–Mg [22], Tm–Mg [23]. The Pr–Mg system has also been carefully studied by using the Smith thermal analysis technique [15].

Other binary R-Mg phase diagrams are reported in literature: Sc–Mg [24, 25], Y–Mg [26, 27], La–Mg [28, 29], Ce–Mg [28, 30], Gd–Mg [29, 31], Eu–Mg [32] and Yb–Mg [33].

Several smooth trends have been observed to occur in R–Mg series of intermetallic compounds for different properties (compound formation, temperatures of the invariant equilibria, etc.) as a function of the atomic number of the rare earth element involved. These trends, moreover, have also been used satisfactorily to optimise data and to predict, particularly in the case of Mg alloys, the phase equilibria in specific ternary systems involving Mg (such as R–R'–Mg systems formed by Mg with two rare earth metals [27, 34–37]).

Many Mg–X–R ternary systems (*X*=element of the Periodic Table) have also been investigated. Data on these are reported in collections of ternary phase diagrams such as 'Multicomponent Alloy Constitution Bibliography' [38], 'Ternary Alloys' [39, 40], 'Handbook of Ternary Alloy Phase Diagrams' [41].

Among the most recent contributions to the knowledge of the behaviour of metallic systems involving magnesium and rare earth metals, we can mention the paper by Tsai *et al.* [42] on Mg–Zn–Y phase diagram, involving quasi-crystals, and a paper by Hu *et al.* [43], in which by using the analytical modified embedded atom method (MEAM), a number of thermodynamic properties of Mg–R alloys have been calculated.

The binary Mg–Ce system was investigated previously by different researchers [28, 44, 45]. A detailed assessment of the system is presented by Nayeb-Hashemi and Clark [30], along with a thermodynamic evaluation and a theoretical prediction, based on the interpolation of experimental data. The assessed diagram is mainly based on the work by Vogel and Heumann [28], even if the more complex regions have been subjected to further investigations. In particular, the Mg-rich zone has been examined by Wood and Cramer [45] using XRD, metallographic and DTA analyses. In spite of this, Nayeb-Hashemi and Clark [30] state that 'a better investigation on 10 at% Ce zone could be opportune'. Up to now, no new experimental studies exist on the Mg–Ce system.

In the assessed Mg–Ce phase diagram the following phases are reported and the following invariant temperatures suggested:

MgCe (cubic, cP2-CsCl type, peritectic formation at 711°C), Mg_2Ce (cubic, cF24-Cu_2Mg type, peritectic formation at 750°C, followed by eutectoidal decomposition at 615°C), Mg_3Ce (cubic, cF16-BiF_3 type, melting point at 796°C), $Mg_{41}Ce_5$ (tetragonal, tI92- $Mg_{41}Ce_5$ type, peritectic formation at 635°C), $Mg_{10.3}Ce$ (with $Ni_{17}Th_2$ structure, peritectic formation at 621°C, followed by eutectoidal decomposi-

tion at 611°C) and finally $Mg_{12}Ce$, (two forms, $Mg_{12}Ce$(I), tetragonal, tI26-$ThMn_{12}$, and $Mg_{12}Ce$(II), orthorhombic, oI338-$Mg_{12}Ce$(II) type, peritectic formation at 616°C).

If we consider the very small temperature difference between the reactions in the region of 10 at% Ce (occurring from 610 to 630°C), a check by a more sensitive technique, like the Smith thermal analysis, can be effective, along with a further investigation of the modality of formation of the Mg-rich phases, by means of phase analysis techniques, typically X-ray diffraction analysis and electron probe microanalysis.

In addition to the Mg-rich side, the Ce-rich region, drawn in the assessed diagram with dashed lines because of the lack of thermal data (except for the invariant temperatures and the liquidus line) has also been investigated. The solvus line itself, drawn solid in [30], was obtained by using X-ray diffraction data.

It should also be considered that many of the literature data were obtained on alloys prepared from low purity elements: this may have greatly affected the stability of the phases and the values of the lattice parameters.

Experimental

Sample preparation

Small pieces of magnesium (99.99 mass% purity) and cerium (99.9 mass% purity), both supplied by Koch Chemicals Ltd., Hertford, UK, were introduced into the opened, inverted crucibles (Fig. 1) and then sealed by tungsten inert gas (TIG) welding.

The alloys were repeatedly melted in an induction furnace under flowing argon, in order to homogenise the samples, performing the last melting with the thermocouple well on the upper side of the crucible, i.e. the same position assumed during the measurements, and finally cooled down by switching off the furnace. As it is important that the measuring thermocouple be completely surrounded by the sample, it is necessary to have the volume inside the crucible filled as much as possible with the alloy. This enhances the response of the Smith apparatus for better reproducibility.

Before carrying out each thermal run, both on heating and on cooling, the samples were annealed inside the Smith furnace for some hours so as to have the sample completely uniform. On the other hand, it has been noticed that excessively long annealing times make the crystals of the phase too big; this makes the method less sensitive.

Nine alloys were prepared and examined by Smith thermal analysis. Eight of them have a composition between 4.5 and 10 at% Ce, whereas the ninth belongs to the Ce-rich side so as to localise the curve related to the solvus and other monovariant equilibria.

Experimental apparatus

The Smith thermal analysis apparatus used in this work is the same as that used at the Manchester Materials Science Centre (UK) and is fully described in previous papers [11, 15], together with the details for sample temperature measurements and data log-

ging equipment. The special-shaped tantalum crucibles, to be sealed by TIG welding, used for the preparation of Mg–Ce alloys and the subsequent thermal analysis measurements, have also been described in [15], where their use was introduced for the investigation of the Mg–Pr system. Their use with Mg–Ce alloys, very reactive and with high vapour pressure, was essential to avoid a change in the alloy composition and damage of the apparatus caused by evaporation of the metals. The measurements were performed in a flux of inert gas (Ar) to prevent the oxidation of the crucibles at high temperatures.

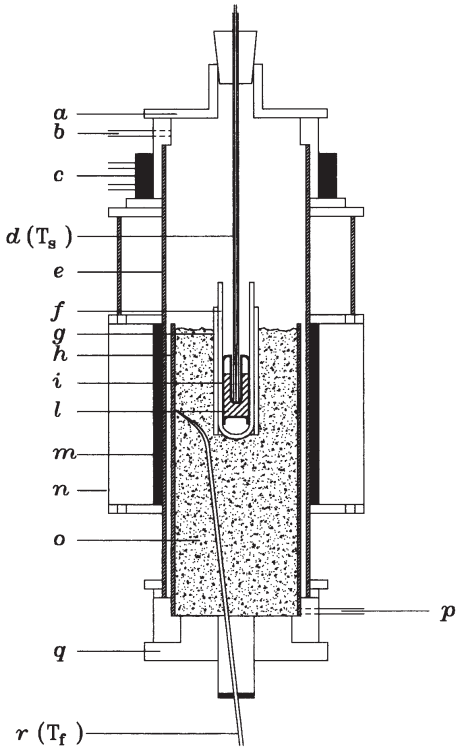

Fig. 1 Schematic drawing of the Smith thermal analysis rig. The special-shaped tantalum crucible is also shown inside the central silica tube
a – top end-cap; b – argon gas out; c – chilled water jacket; d – thermocouple sheath; e – alumina furnace tube; f – central silica tube; g – silica guide tube; h – inner alumina tube; i – tantalum crucible; l – sample; m – heating element; n – furnace case; o – ceramic wool; p – argon gas in; q – bottom end-cap; r – furnace thermocouple

Figure 1 shows a schematic drawing of the Smith thermal analysis rig with the special–shaped tantalum crucible inside the inner alumina tube.

The calibration of the measurement thermocouple was done by reference to the melting points of pure metals (In, Sn, Bi, Pb, Zn, Al).

After the thermal runs the alloys were examined by using several techniques, such as XRD powder diffraction (Debye method, CuK_α radiation), optical (LOM) and scanning electron microscopy (SEM), and electron probe microanalysis (EPMA). Details on the use of these techniques to investigate rare earth alloys have been reported in previous papers [17, 22].

Results and discussion

The investigated alloy compositions are listed in Table 1, along with the thermal data values. Notice that the latter are a result of repeated thermal runs, performed both on heating and on cooling so as to discard possible instrumental errors due to the sensitivity of the method. Figure 2 reports the phase diagram according to the assessment by Nayeb-Hashemi and Clark [30]; in the lower part of the drawing the enlargement of the phase equilibria around 10 at% Ce is shown. The experimental values obtained in the present work, indicated by black circles, are superimposed.

Table 1 Selected Mg–Ce alloys prepared and analysed by Smith thermal method

Sample number	Nominal composition/at% Ce	Thermal effects[a]/°C
1	4.5	601.7 (*L*) 589.6
2	6.0	606.5 (*L*) 590.0
3	6.5 (from EPMA)	611.5 (*L*) 591.4
4	7.5	614.1 (*L*) 610.3 591.6
5	8.0	618.3 (*L*) 615.1 613.5
6	8.2	619.0 (*L*) 615.6 609.6
7	9.0	623.1 (*L*) 616.6 611.7
8	10	639.8 (*L*) 623.5 613.6
9	94	789.4 (*L*) 775.4 660.3 584.7 431.9

[a]Averaged values among the heating and cooling runs; *L*=liquidus

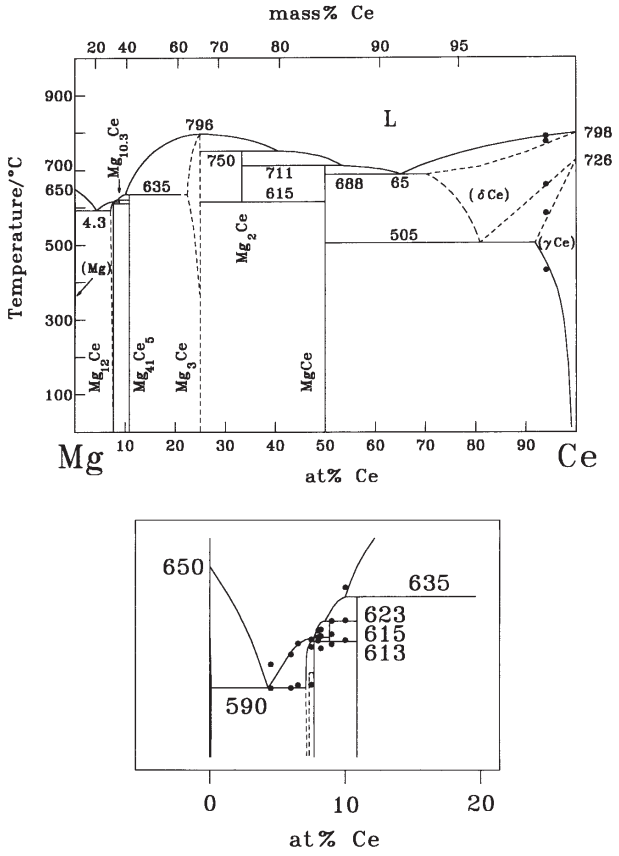

Fig. 2 Mg–Ce system; upper part: Mg–Ce phase diagram as presented in [30]; lower part: enlarged Mg-rich region. The Smith thermal analysis data obtained in this work are superimposed in both drawings (full circles)

The results obtained for the Ce-rich sample confirm the position of the monovariant curves, partly inferred in literature from XRD and metallographic data (Fig. 2). This determination needed several measurement runs, because the intersection of these curves by an isopleth does not correspond to a thermal arrest, but only to a slope change of the rate *vs.* time curve giving low reproducibility.

As for the Mg-rich alloys, our data fall within the composition range suggested in [30]. Table 2 collects the coordinates of the invariant reactions on the Mg-rich side of the Mg–Ce system as obtained in this work (and compared with literature value).

For the thermal effects between 610 and 630°C concerning the eutectoidal decomposition of $Mg_{10.3}Ce$ (613°C), the peritectic formation of $Mg_{12}Ce$ (615°C) and the peritectic formation of $Mg_{10.3}Ce$ (623°C), the values now obtained are in very good agreement with those by Wood and Cramer [45] but with a higher precision (±1°). In [45], these results were obtained from partially resolved peaks.

Table 2 Mg–Ce system: invariant reactions of the Mg-rich side

Reaction	Reaction type	Composition of the phases/at% Ce			*T*/°C this work	*T*/°C literature
$L \leftrightarrow Mg$	melting point		0		–	650
$L \leftrightarrow (Mg)+Mg_{12}Ce$	eutectic	4.3	0.09	7.7	590±1	592
$L+Mg_{10.3}Ce \leftrightarrow Mg_{12}Ce$	peritectic	~7.5	8.8_5	7.7	615±1	616
$L+Mg_{41}Ce_5 \leftrightarrow Mg_{10.3}Ce$	peritectic	~8.5	10.9	8.8	623±1	621
$Mg_{10.3}Ce \leftrightarrow Mg_{12}Ce+Mg_{41}Ce_5$	eutectoid	8.8	7.7	10.9	613±1	611
$L+Mg_3Ce \leftrightarrow Mg_{41}Ce_5$	peritectic	~10	~23	10.9	–	635

As for the $Mg_{41}Ce_5$ phase a peritectic reaction at 635°C was suggested in literature [45], by using temperature data obtained only from the heating runs. The results now obtained from the sample at 10 at% Ce indicate that the peritectic formation temperature of this phase could be a few degrees higher.

The temperature of the Mg-rich eutectic was found at 590°C (literature value 592°C).

The metallographic examination was performed by LOM and SEM analyses and confirms the formation mechanisms of the Mg-rich phases. The compositions of the phases present in every sample are in agreement with the compound stoichiometries reported in literature, and the relevant global compositions were checked by EPMA analysis. The check of the global composition permits us to ascertain the homogeneity of the samples and possible composition changes. Actually, sample #3 revealed, after EPMA analysis, a composition different from the theoretical one, so its thermal values were assigned to the corresponding experimental composition.

Figure 3 shows the typical micrographic appearance of a Mg–6.0 at% Ce alloy.

Table 3 summarises the crystal structure and the lattice parameters of the phases pertaining to the Mg–Ce system both from this work and from literature.

Fig. 3 Backscattered electron (BSE) micrograph of a Mg–6.0 at% Ce alloy, after Smith thermal analysis runs
$Mg_{12}Ce$ phase (white) surrounded by eutectic structure (formed by Mg solid solution and $Mg_{12}Ce$)

Table 3 Mg–Ce crystal structure and lattice parameters data

Phase/nominal compositions	at% Ce	Structure type	Sample composition/ at% Ce	Lattice parameters/ pm		Comments	References
				a	c		
(Mg)	0 to 0.09	hP2-Mg		320.93	521.07		[46]
			4.5	321.2	521.4		this work
			6.0	321.1	521.8		this work
$Mg_{12}Ce$ (I)	7.69	tI26-$Mn_{12}Th$		1033	596		[45]
				1032	596		this work
$Mg_{12}Ce$ (II)	7.69	oI338-$Mg_{12}Ce$ (II)		1033	7750		[45]
$Mg_{10.3}Ce$	8.85	hP38-$Ni_{17}Th_2$		1031	1032		[45]
			9.0	1035	1036	two-phase sample	this work
			10.0	1034	1032	two-phase sample	this work
$Mg_{41}Ce_5$	10.87	tI92-$Mg_{41}Ce_5$		1454	1028		[45]
			9.0	1456	1025	two-phase sample	this work
			10.0	1460	1031	two-phase sample	this work
Mg_3Ce	? to 25	cF16-BiF_3		743.6			[28]
Mg_2Ce	33.33	cF24-Cu_2Mg		870			[28]
MgCe	50.00	cP2-CsCl		392.4			[30]
(δ-Ce)	? to 100	cI2-W		412			[46]
(γ-Ce)	91.8 to 100	cF4-Cu		516.1			[46]
βCe –		hP4-αLa		368.10	1185.7		[46]
αCe –		cF4-Cu		485			[46]

Conclusions

In conclusion, it is possible to state that the Smith method, which proves to be very accurate in the precise determination of close effects, allowed us to confirm the Mg-rich part of the Mg–Ce phase diagram in which a number of intermetallic phases with peritectic formation is present. On the other hand, information about the solidus and solvus lines (to which very small thermal effects are generally associated) of the Ce-rich region of the diagram have also been obtained. Thus, it can be highlighted that, in the field of metallic phase diagrams, combination of the DTA technique, generally faster in the investigation of a large temperature interval, and the Smith method may be especially beneficial.

* * *

This work is performed in the framework of the Italian Progetto Finalizzato 'Materiali Speciali per Tecnologie Avanzate II', (PF MSTA II), whose support is acknowledged with thanks.

References

1 W. Hume-Rothery, J. W. Christian and W. B. Pearson, 'Metallurgical Equilibrium Diagrams', London, The Institute of Physics, Chapman & Hall Ltd., London 1953.
2 F. N. Rhines, 'Phase Diagrams in Metallurgy – Their Development and Application', McGraw-Hill Book Company, Inc., (1956), p. 301.
3 W. W. Wendlandt and L. W. Collins, 'Thermal Analysis', Dowden, Hutchinson & Ross, Inc., Stroudsburg (PA), USA 1976.
4 R. Ferro, A. Saccone, S. Delfino, D. Macciò, F. H. Hayes and J. A. J. Robinson, J. Mining and Metallurgy, 35 (1999) 315.
5 D. S. Evans and A. Prince, J. Less-Common Met., 58 (1982) 199.
6 C. S. Smith, Trans. Amer. Inst. Met. Eng., 137 (1940) 236.
7 F. H. Hayes, R. D. Longbottom, E. Ahmed and G. Chen, J. Phase Equilibria, 14 (1993) 425.
8 F. H. Hayes, W. T. Chao and J. A. J. Robinson, J. Thermal Anal., 42 (1994) 745.
9 F. H. Hayes and W. T. Chao, in: 'User aspects of Phase diagrams', F. H. Hayes (Ed.), Institute of Metals, London 1991, p. 121.
10 F. Weitzer, P. Rogl, F. H. Hayes and J. A. J. Robinson, Werkstoff Woche '95, Materialwissenschaftliche Grundlagen, Eds. F. Aldinger and H. Murghrabi, Published by Deutsche Gesellschaft für Materialkunde, Frankfurt 1997. p. 185.
11 F. H. Hayes, J. A. J. Robinson, and W. T. Chao, in 'Experimental Methods of Phase Diagram Determination', J. E. Morral, R. S. Schiffman and S. M. Merchant (Eds.), Publishers: TMS, Warrendale, PA, USA 1994, p. 101.
12 P. J. Horrocks, N. D. Moulson and F. H. Hayes, Thermochim. Acta, 204 (1992) 25.
13 P. J. Horrocks, 'Phase Diagram and Thermodynamics of the Ag–Cd–In Ternary Alloy Systems', Ph. D. Thesis, UMIST 1991.
14 J. A. J. Robinson, 'Phase Equilibria Studies in Some Ternary Ag–Cd–In Alloys', M. Sc. Thesis, UMIST 1993.
15 A. Saccone, D. Macciò, J. A. J. Robinson, F. H. Hayes and R. Ferro, J. Alloys and Compounds, 317/318 (2001) 497.

16 S. Delfino, A. Saccone and R. Ferro, Met. Trans., 21A (1990) 2109.
17 A. Saccone, A. M. Cardinale, S. Delfino and R. Ferro, Intermetallics, 1 (1993) 151.
18 A. Saccone, S. Delfino, G. Borzone and R. Ferro, J. Less-Common Metals, 154 (1989) 47.
19 A. Saccone, S. Delfino, D. Macciò and R. Ferro, J. Phase Equilibria, 14 (1993) 479.
20 A. Saccone, S. Delfino, D. Macciò and R. Ferro, Z. Metallkde., 82 (1991) 568.
21 A. Saccone, S. Delfino, D. Macciò and R. Ferro, J. Phase Equilibria, 14 (1993) 280.
22 A. Saccone, S. Delfino, D. Macciò and R. Ferro, Metall. Trans. A, 23A (1992) 1005.
23 A. Saccone, D. Macciò, S. Delfino and R. Ferro, J. Alloys and Compounds, 220 (1995) 161.
24 L. N. Komissarova and B. I. Pokrovskii, Russ. J. Inorg. Chem., 9 (1964) 1233.
25 A. Pisch, R. Schmid-Fetzer, G. Cacciamani, P. Riani, A. Saccone and R. Ferro, Z. Metallkde., 89 (1998) 474.
26 E. D. Gibson and O. N. Carlson, Trans AIME 52 (1960) 1084.
27 M. Giovannini, A. Saccone, R. Marazza and R. Ferro, Metall. Mater. Trans. A, 26A (1995) 5.
28 R. Vogel and T. Heumann, Z. Metallkde., 38 (1947) 1.
29 P. Manfrinetti and K. A. Gschneidner Jr., J. Less-Common Metals, 123 (1986) 267.
30 A. A. Nayeb-Hashemi and J. B. Clark, 'Phase Diagrams of Binary Magnesium Alloys', ASM International, Metals Park, OH 1988.
31 G. Cacciamani, A. Saccone, G. Borzone, S. Delfino and R. Ferro, Thermochim. Acta, 199 (1992) 17.
32 W. Mühlpfordt and W. Klemm, J. Less-Common Metals, 17 (1969) 127.
33 O. D. McMasters and K. A. Gschneidner Jr., J. Less-Common Metals, 8 (1965) 289.
34 M. Giovannini, A. Saccone and R. Ferro, J. Alloys and Compounds, 220 (1995) 167.
35 H. Flandorfer, M. Giovannini, A. Saccone, P. Rogl and R. Ferro, Metall. Mater. Trans. A, 28A (1997) 265.
36 M. Giovannini, A. Saccone, H. Flandorfer, P. Rogl and R. Ferro, Z. Metallkde., 88 (1997) 372.
37 M. Giovannini, A. Saccone and R. Ferro, Intermetallics, 7 (1999) 909.
38 A. Prince, 'Multicomponent Alloy Constitution Bibliography 1955–1973', The Metals Society, London 1978.
39 G. Effenberg, F. Aldinger and L. Rokhlin (Eds.), 'Ternary Alloys. A Comprehensive Compendium of Evaluated Constitutional Data and Phase Diagrams', VCH, Germany, Weinheim 1999, Vol. 16.
40 G. Effenberg, F. Aldinger and P. Rogl (Eds.), 'Ternary Alloys. A Comprehensive Compendium of Evaluated Constitutional Data and Phase Diagrams', VCH, Germany, Weinheim 2000, Vol. 17.
41 P. Villars, A. Prince and H. Okamoto (Eds.) 'Handbook of Ternary Alloy Phase Diagrams', ASM International, (1995), Vol. 1-10.
42 A. P. Tsai, Y. Murakami and A. Niikura, Phil. Mag., Phys. Cond. Matter, Struct. Defect, Mech. Prop., 80 (2000) 1043.
43 W. Y. Hu, H. D. Xu, X. L. Shu, X. J. Yuan, B. X. Bao and B. W. Zhang, J. Phys. D Appl. Phys., 33 (2000) 711.
44 L. Haughton and T. H. Schofield, J. Inst. Met., 60 (1937) 339.
45 D. H. Wood and E. M. Cramer, J. Less-Common Met., 9 (1965) 321.
46 T. B. Massalski, H. Okamoto, P. R. Subramanian and L. Kacprzak (Eds), 'Binary Alloy Phase Diagrams', 2nd edition, ASM International, (1990), Vol. 1.